

1 **Monitoring fibrillation in the mechanical production of lignocellulosic** 2 **micro/nanofibers from bleached spruce thermomechanical pulp**

3 Ferran Serra-Parareda ^{1,*}, Quim Tarrés ^{1,2}, M. Àngels Pèlach ¹, Pere Mutjé ^{1,2}, A. Balea ³, M.C.
4 Monte ³, C. Negro ³, Marc Delgado-Aguilar ¹

5 ¹ LEPAMAP Research group, University of Girona, Maria Aurèlia Capmany, 6, 17003 Girona,
6 Spain

7 ² Chair on Sustainable Industrial Processes, University of Girona, Maria Aurèlia Capmany, 6,
8 17003 Girona, Spain

9 ³ Department of Chemical Engineering and Materials, University Complutense of Madrid,
10 Avda Complutense s/n, 28040, Madrid, Spain.

11 * Corresponding author: ferran.serrap@udg.edu

12 **Abstract**

13 The present work aims at assessing the main characteristics of lignocellulosic micro/nanofibers
14 (LCMNF) from bleached thermomechanical pulp (BTMP) from spruce while glimpsing the
15 suitability of cationic demand (CD) as effective monitoring parameter of the fibrillation process.
16 For this, BTMP was mechanically refined at different times in a Valley beater, aiming at
17 determining the required refining time and fiber length to be later fibrillated in a high-pressure
18 homogenizer. It was found that 150 min treatment is required to avoid clogging in the pressure
19 chambers of the homogenizer. The mechanically treated BTMP was gradually passed through a
20 high-pressure homogenizer, leading to four LCMNF with different fibrillation degree. The main
21 characteristics of the LCMNF were determined, as well as the effect that high-pressure
22 homogenization may generate onto the LCMNF structure. It was observed that CD is a robust
23 parameter to monitor the fibrillation process, as it is a good indicator of the LCMNF
24 characteristics. In addition, it was found that WRV may not be a good indicator of the extent of
25 fibrillation for LCMNF, as the lignin content varies with the homogenization intensity. Finally,
26 the limitations of CD as monitoring parameter and perspectives on this regard are provided to the
27 reader.

28 *Keywords: Lignocellulosic micro-nanofibers; lignin; Cationic Demand*

29 **1 Introduction**

30 Over the past few years, cellulose has gained prominence as a nanostructured material for the
31 development of products with low environmental impact, mainly instigated by the need to reduce
32 the dependence on fossil resources [1–3]. In addition to its sustainable character, cellulose
33 nanofibers (CNF) present high specific surface area and aspect ratio (length/diameter), excellent

34 mechanical properties, low toxicity, low density and good dimensional stability [4,5]. These
35 properties make CNF a highly attractive material to substitute synthetic materials and to improve
36 the recyclability and biodegradability of products [6].

37 However, up to date, the production and commercialization of CNF-based products has been
38 limited by several factors [7,8]. A major obstacle to be overcome are the elevated processing costs
39 related to expensive pretreatments involving the use of chemicals and enzymes [9]. For instance,
40 TEMPO catalyst has been reported to be expensive [10] and difficult to recover [11,12]. Besides,
41 chemical pretreatments are also associated with human health effects and environmental issues
42 since they require the employment of toxic reagents [13]. Chemical pretreatments also cause
43 excessive depolymerization of fiber components and contribute to the thermal instability of the
44 fibers, finally dealing with great struggles in both recycling and regeneration processes [14,15].
45 Besides, the enzymatic pretreatment route is more environmentally friendly than the chemical
46 one, but facing the difficulty in its application owing to the high cost of enzymes and long
47 processing time required for cellulose degradation [16,17].

48 From a technical viewpoint, the abundance of hydroxyl groups at the CNF's surface highly
49 increases their water uptake and viscosity in aqueous suspensions, which could finally decrease
50 their industrial performance in unit operations like dewatering, pumping and dispersion, among
51 others [18]. Additionally, the development of efficient drying systems allowing their dispersion
52 back into a new solvent avoiding the hornification phenomena is still a challenge nowadays [19].

53 Such concerns can be avoided or at least mitigated using lignin containing pulps as raw material
54 in substitution to those highly delignified chemical ones [20,21]. So far, the production of lignin
55 containing nanofibers has been based on the use of unbleached chemical pulps with residual lignin
56 content [22–24]. However, high yield pulps with elevated lignin content offer a sustainable low-
57 cost alternative to unbleached chemical pulps. The main advantage of high yield pulping is that it
58 produces much higher yields (> 90 %) than chemical pulping (< 50 %) [25]. These high yield
59 pulps can be produced by means of mechanical defibration methods (mechanical pulp),
60 sometimes combined with elevated temperatures (thermomechanical pulp), and the use of low
61 amounts of chemicals (chemo-thermomechanical pulp) to improve the efficiency of fibers
62 separation. Within these processes, chemo-thermomechanical pulps require the use of chemicals
63 and offer lower yields than mechanical and thermomechanical ones. Besides, thermomechanical
64 pulp fibers offer improved properties in comparison to mechanical pulps, and still retain the high
65 yield and cost effectiveness of mechanical pulps [26]. In this context, spruce wood is widely
66 known to be an interesting resource for thermomechanical pulp production, as they usually
67 present reasonably higher mechanical properties than other softwood pulps. These superior
68 properties, apart from the presumably higher intrinsic properties of spruce fibers compared to the

69 rest of softwood sources, may come from the low extractives content [27]. The thermomechanical
70 treatment can be followed by a soft bleaching step to increase pulp brightness and remove some
71 surface impurities, leading to a bleached thermomechanical pulp (BTMP).

72 As mentioned before, thermomechanical pulping offers high processing yields, which means that
73 the chemical composition of the raw material is not significantly affected. Hence, the content of
74 lignin and hemicelluloses is expected to be high in these pulps. It has been reported that lignin
75 and hemicellulose could ease the mechanical fibrillation efficiency of fiber bundles into
76 nanofibers, resulting in a reduction of the energy consumption and better processability [28]. In
77 fact, most delignified pulps are pretreated by means of chemical and enzymatic processes instead
78 of mechanical pretreatment to enable the correct fibrillation of the pulp, whereas the presence of
79 lignin in high yield pulps offer the possibility of replacing those expensive pretreatments by
80 mechanical ones. Amongst possible mechanical pretreatments, the use of the PFI mill and Valley
81 beater has been widely recognized by researchers [29,30]. While PFI mills boost fibers' internal
82 destructuration by replacing the fiber-to-fiber bonds by fiber-to-water bonds, Valley beaters
83 produce larger quantities of fines and are more effective on reducing fibers' length through cutting
84 action. Although in the field of the paper and board such cutting effect has been considered
85 harmful for the paper strength, in the field of nanofibers reducing fibers' length is crucial to enable
86 the correct fibrillation in the homogenizer and reduce the clogging tendency. This idea was
87 supported by Turbak et al., (1983) who claimed that precut fibers at the length range of 600 to
88 700 μm could ease the fibers destructuring [31]. Hence, the Valley beater route would be a more
89 appropriate choice to pretreat mechanically the fibers prior to homogenization.

90 Another factor limiting the industrialization of CNF is the lack of fast and robust characterization
91 method to perform an efficient quality control along the production chain. Although progress has
92 been made in this field, there is an absence of process-adapted characterization tools that allow a
93 fast and reliable approach of the suspension quality in a cost-effective way. In addition, the
94 selection of an appropriate process variable is usually difficult. The use of optical methods has
95 been investigated to determine the quality of nanocellulose, though, the observation may not be
96 representative of the whole suspension [32]. In addition, the incorporation of high-resolution
97 microscopy tools in the production chain of nanocellulose can be difficult. Instead, the
98 determination of the nanofibers' quality via a multiparameter analysis has been proposed.
99 Desmaisons et al., (2017) [33] proposed a multi-criteria method that enabled the obtention of a
100 single quantitative grade that allowed the monitorization of the production of nanocellulose.
101 Though, the analysis required the production of nanopapers for the determination of the Young's
102 modulus, generating a critical lag between process and characterization. The WRV has been also
103 proposed to determine the degree of fibrillation, though, still on the way to confirm its validity
104 with high lignin content pulps. Overall, proposing methods to monitor the fibrillation of the

105 suspensions is required to ease the scale-up production of nanofibers. As a result, in this work the
106 cationic demand (CD) parameter is proposed as a reliable and fast method to monitor the
107 mechanical fibrillation of lignocellulosic micro-nanofibers.

108 In terms of applicability, nanofibers have been used in sectors such as paper, automotive, paints
109 and coatings, composites, textiles, cement and concrete and pharmaceutical [2,11,34–39].
110 Nonetheless, the presence of lignin in nanofibers can give rise to the development of novel
111 nanomaterials with chemical, mechanical and physical properties differing from the traditional
112 CNF. The partially hydrophobic character of lignin can give rise to new opportunities in
113 biocomposite materials [40], acting as compatibilizer with hydrophobic matrixes, oil-water
114 stabilization aerogels [41] and medium density fiberboards (MDF) [42]. Lignin can as well act as
115 natural binder in nanopapers, reducing the porosity and providing improved barrier properties
116 [23]. There are also opportunities in the biomedical field as an antioxidant, antidiabetic and
117 antimicrobial material [43,44]. Among these range of applications, the use of nanofibers as
118 strengthening additive in the paper and board sector has been widely recognized. According to a
119 recent report by Future Markets Inc. [45], the paper and board sector currently represents the 74
120 % of the global demand for cellulose nanofibers with 6,998 tons. The demand of CNF in this
121 sector is far from the second and third most demanded fields, which are the field of composites
122 (12 %) and rheological modifiers (11 %). Furthermore, the use of nanofibers in the paper and
123 board field is expected to increase exponentially in upcoming years, reaching a demand up to
124 38,643 tons of CNF by the year 2030, which corresponds to an increase by the 452 %. For this
125 reason, along with an increasing market pressure for quality improvements and stricter quality
126 standards, there is a need to instigate the production of nanofibers in this sector making it
127 economically attractive and feasible to implement at large scale.

128 Overall, the present work aims to produce high lignin content micro-nanofibers using a high yield
129 pulp as raw material and to study the influence of the refining using a Valley beater and
130 homogenization process on the quality of the final suspensions. In addition, the present work also
131 reveals the suitability of cationic demand as robust monitoring parameter of the fibrillation
132 process, while detailing the main limitations and few perspectives on this regard.

133 **2 Experimental**

134 **2.1 Materials**

135 Bleached spruce thermomechanical pulp (BTMP) was provided by Norske Skog Saugbrugs
136 (Halden, Norway) and was used for the preparation of lignocellulosic micro-nanofibers. All
137 chemical reagents used for the complete characterization of the micro-nanofibers were supplied
138 by Sigma Aldrich and were used as received.

139 2.2 Methods

140 2.2.1 Characterization of the BTMP

141 The chemical composition of the pulp was evaluated according to TAPPI standard methods.
142 Fibers were dried prior to analysis at 105 °C for 24h, as required by TAPPI T264. Then, the
143 extractives content was measured by means of ethanol-toluene Soxhlet extraction according to
144 TAPPI T204. Ash and lignin were determined according to TAPPI T211 and TAPPI T22,
145 respectively. The content of cellulose and hemicellulose was determined by high performance
146 anion exchange chromatography (HPAEC). Further details of this methodology were reported by
147 [46].

148 Pulp drainability was measured according to ISO 5267/1 and expressed as Schopper – Riegler
149 degree (°SR) and as Canadian Standard Freeness (CSF), which was directly converted from °SR
150 to CSF. The morphological analysis was performed using a MorFi Compact Analyzer (TechPap,
151 Grenoble, France) equipped with a CCD video camera. About 30,000 fibers were analyzed by the
152 software MorFi v9.2 and, among other parameters, the mean fiber length (l_w^F), mean fiber
153 diameter (d^F) and fines content measured in length (f_l) were determined. Those fibers shorter than
154 76 μm were considered as fines by the software. The fines content in weight (f_w) was determined
155 by passing the pulp suspension several times through a 200-mesh filter and recovering the filtrate,
156 which was then oven-dried at 105 °C until constant weight and referred to the initial dry weight
157 of pulp. The specific surface area of the pulp was determined by means of dye Congo Red
158 adsorption methodology. Such methodology will be later specified during the characterization of
159 the micro-nanofibers.

160 2.2.2 Production of lignocellulosic micro-nanofibers (LCMNF)

161 BTMP was previously disintegrated in a 50 L-pulper equipped with a helicoidal rotor at the
162 bottom at 5 wt.% consistency. Then, the pulp was diluted until reaching a consistency of 2 wt%
163 and mechanically refined in a Valley beater using the 500 g weight. Residence times for the
164 refining operations were set at 50, 100 and 150 min. The appropriate refining time was chosen
165 depending on the aptitude of the suspension to be properly treated in the high-pressure
166 homogenizer (HPH).

167 The pretreated suspension was passed through a high-pressure homogenizer (NS1001L PANDA
168 2000-GEA, GEA NiroSoavi, Italy) by progressively increasing the number of passes and
169 pressure. Finally, a mix of both micro and nano fibers was obtained and referred to as
170 lignocellulosic micro-nanofibers (LCMNF). Samples were separated at different stages of the
171 fibrillation process, leading to LCMNF 1, LCMNF 2, LCMNF 3 and LCMNF 4, as reflected in
172 Table 1.

173 **[TABLE 1 ABOUT HERE]**

174 The reason behind the suspensions were subjected to progressive fibrillation is that a sudden
175 increase of the shearing forces can negatively affect the properties of the nanofibers due to the
176 degradation of the fibrils and, thus, a progressive increase of the pressure would avoid damaging
177 the nanofibers [47].

178 2.2.3 Characterization of the lignocellulosic micro-nanofibers (LCMNF)

179 The yield of nanofibrillation was evaluated by centrifuging 0.1 g (dry weight) of LCMNF from a
180 suspension at 1 wt.% consistency. The nanofibrillated fraction contained in the supernatant was
181 isolated from the non-nanofibrillated, which was assumed to be retained in the sediment. The
182 recovered sediment was then oven-dried until constant weight. The yield of nanofibrillation was
183 then calculated according to equation 1.

$$184 \text{ Yield of nanofibrillation (\%)} = \left(1 - \frac{m_{ds}}{m_s}\right) \cdot 100 \quad (1)$$

184 Where m_{ds} and m_s are the mass of dry sediment and initial dry sample, respectively.

185 The transmittance of the LCMNF suspensions was measured via a UV-Vis Shimadzu
186 spectrophotometer UV-160A set in the range between 400 and 800 nm. Distilled water was used
187 as reference and background.

188 The morphology of the obtained LCMNF was assessed by means of Field Emission Scanning
189 Electron Microscopy (FE-SEM) using a Hitachi S-3000 microscope (Hitachi Europe S.A.,
190 Barcelona, Spain) operating at 12 kV of accelerating voltage.

191 The carboxyl content (CC), which may not be significantly affected by the refining treatment,
192 was determined by conductimetric titration, as previously reported [48]. Cationic demand (CD)
193 was determined by back titration in a particle charge detector (Mütek PCD 04, BTG), as it has
194 been extensively described in other works [10]. According to the supplier, the molecular weight
195 (Mw) of polyDADMAC accounted for 107 kDa.

196 The water retention value (WRV) was measured by means of centrifuging the LCMNF
197 suspensions in bottles equipped with a nitrocellulose membrane (0.22 μm of pore size), which
198 can separate the non-bonded water out of the LCMNF suspension. Suspensions were centrifuged
199 for 30 min at 2400 rpm (452 G-force). The wet cake that was formed on the top of the
200 nitrocellulose membrane was then collected, weighted, and dried at 105 °C until constant weight.
201 The WRV was calculated referring the amount of water in the wet cake per dry gram of sample
202 [49].

203 The degree of polymerization (DP) was determined by means of intrinsic viscosity measurements
204 for dissolved LCMNF in cupri-ethylenediamine according to UNE-ISO 5351 standard. The
205 correlation between intrinsic viscosity and DP was given by the Mark-Howink-Sakurada equation

206 and values for K and a , constants from the equation that depend on the polymer-solvent system,
207 were set at 2.28 and 0.76, respectively [29].

208 Specific surface area (SSA) was determined by means of two different methods. On the one hand,
209 it was estimated from the CC and CD, considering the interactions between CNF and the added
210 cationic polymer (polyDADMAC). Details from this method have been previously published by
211 the authors and it has been reported to provide reliable values of, at least, diameters [46,50]. On
212 the other, SSA was calculated by means of Congo red adsorption isotherms, as described
213 elsewhere [51].

214 Changes on the lignin content and crystallinity of the LCMNF were assessed by means of Klason
215 lignin method and X-ray diffraction (XRD), respectively. For this, the suspensions were vacuum
216 filtered in a modified sheet former equipped with a 0.22 μm nitrocellulose membrane and then
217 dried for 20 min to remove water. Klason lignin of the LCMNF was measured on grinded and
218 dried samples according to TAPPI T22 om-98. The crystallinity index (C.I.) was calculated from
219 an XRD profile on the small pieces of the substrates. The C.I. was obtained from the height ratio
220 between the intensity of the crystalline peak ($I_c - I_{am}$) and total intensity (I_c), as reported by
221 Segal et al., (1959) (equation 2) [52].

$$C.I. (\%) = \frac{I_c - I_{am}}{I_c} \cdot 100 \quad (2)$$

222 3 Results and Discussion

223 3.1 Characterization of the BTMP

224 Aiming at glimpsing the effect of the thermomechanical and soft bleaching process, the chemical
225 composition of the bleached thermomechanical pulp (BTMP) was determined and compared to
226 an unbleached [53] and bleached [54] kraft spruce pulp (UKSP and BKSP, respectively), as
227 reflected in Table 2.

228 [TABLE 2 ABOUT HERE]

229 BTMP exhibited a content of acid insoluble lignin, also known as Klason lignin, a hemicellulose
230 content and a cellulose content of 25.80, 25.40 and 48.35 wt%, respectively. The content of non-
231 structural elements such as extractives and ashes were relatively low for a thermomechanical pulp
232 with values of 0.25 and 0.20 wt%, respectively. Wang et al., (2018) [55] reported a chemical
233 composition for spruce wood (*Picea abies*) of 42.0 wt.% of cellulose, 20.6 wt.% of hemicellulose,
234 28.2 wt.% of Klason lignin, 6.5 wt.% of acid-soluble lignin, and 1.04 wt.% of extractives. Out of
235 these values, one can see that the pulping and bleaching process removed the extractives by more
236 than half from 1.04 to 0.25 wt.%. Besides, the lignin content experienced a smooth decrease from

237 28.2 to 25.8 wt.%, mainly due to the impact of the bleaching process. As a result, the relative
238 content of cellulose and hemicellulose increased with respect to the raw wood from 62.6 to 73.75
239 wt.%. Overall, this indicates that BTMP, although having been submitted to a bleaching step,
240 still presented a relatively high content of lignin and that the whole treatment did not significantly
241 affect the major chemical constituents of wood.

242 Table 2 also shows the chemical composition of UKSP and BKSP for comparison purposes. It
243 becomes apparent that the kraft process significantly decreases the lignin content, accounting for
244 2.23 wt% in the case of the pulp reported by Tutus et al. (2010). In addition, when such pulp is
245 submitted to a bleaching stage (BKSP), the resulting pulp exhibited a lignin content below 0.1
246 wt.%. The degradation of lignin by the kraft and bleaching processes may inevitably lead to the
247 removal of other constituents embedded in the amorphous region of the fibers, mainly
248 hemicellulose and some extractives. The content of hemicellulose in both UKSP and BKSP
249 decreased by less than half in comparison to the BTMP. Finally, the cellulose content increased
250 to values around 90 wt.%.

251 As reported by Jonoobi et al., (2014) [56] the chemical composition of the pulp has a major
252 influence during pulp fibrillation. Specifically, other authors pointed out that lignin has a
253 significant role inhibiting the formation of fibril bundles, which may be beneficial for the
254 fibrillation process [51]. Besides, the hemicellulose content has been also reported to be crucial
255 to avoid the aggregation of the microfibrils and re-agglomeration of the nanofibrillated parts [20].
256 Chaker et al., (2013) [57] exposed that hemicellulose content around 25 wt.% in pulps is optimum
257 to reach the maximum fibrillation efficiency, whereas in pulps exhibiting a hemicellulose content
258 close to 12 wt.% may decrease such efficiency by half. Generally, most chemical pulps, either
259 bleached or unbleached, used to produce cellulose nanofibers exhibit a lower hemicellulose
260 content than the BTMP proposed in the present study [58]. In addition, as there is still a lack of
261 understanding on the role of extractives during pulp fibrillation, it is accepted that this fraction
262 should be reduced to a certain extent to enable its proper fibrillation [59]. Thus, at least in terms
263 of chemical composition, BTMP may be a suitable raw material for LCMNF production, as it will
264 presumably be easy to fibrillate.

265 Although chemical composition has a key role on the fibrillation process, both morphological and
266 physical properties also may be affected during such process. Thus, the main morphological
267 parameters are summarized in Table 3.

268 **[TABLE 3 ABOUT HERE]**

269 BTMP exhibited a mean fiber length and diameter of 1,178 and 29.8 μm , respectively. Both length
270 and diameter are significantly higher than in the case of other pulps used for LCMNF production
271 that may be found in the literature. Indeed, the selected pulp exhibited a higher length to other

272 pulps such as chemical pulps from wheat, vine stems and bleached eucalyptus, but shorter than
273 *pinus radiata* [60–62]. The obtained diameter was significantly higher than in the case of
274 hardwoods, but of the same order of magnitude than softwoods [63]. The morphological analysis
275 also returned an elevated content of fines, which partially explains the high SSA (2.87 m²/g).
276 However, such high surface area may be also explained by the aggressive treatment during
277 pulping, where lignin and other constituents are not dissolved and, thus, the mechanical energy
278 randomly breaks the wood structure increasing the surface fibrillation.

279 3.2 Effect of the refining in a Valley beater on the BTMP characteristics

280 Aiming to increase fibrillation, BTMP was subjected to mechanical refining in a Valley beater
281 prior homogenization, as described in the previous section. The morphology, the DP and the CD
282 of the refined pulps were determined, as well as their aptitude to high-pressure homogenization
283 (Table 4).

284 [TABLE 4 ABOUT HERE]

285 After 50, 100 and 150 min treatment, fiber length (l_w^F) decreased to 1,064, 790 and 682 μm ,
286 respectively, representing a reduction of 42 % at 150 min. In fact, fiber length decreased linearly
287 with the pretreatment time with a correlation factor of $R^2 = 0.967$. These results are consistent
288 with those reported by Turbak et al., (1983) [31], where the need of reducing fiber length to a
289 range between 600 and 700 μm can enhance pulp fibrillation during high-pressure
290 homogenization. The decrease on the fiber length was also observed in the DP, which decreased
291 from 3,250 to 2,540 after 150 min treatment. On the contrary, the diameter of the BTMP fibers
292 was not significantly affected, indicating that fiber bundles were not successfully separated, which
293 is something expectable from such kind of mechanical treatments.

294 The mechanical refining also increased the fines content, both in length and in weight. After 150
295 min treatment, the amount of fines in length accounted for 79.5 %, while the mass fraction of
296 fines was 40.6 %. The morphological analysis, conducted by the MorFi equipment, does not
297 consider the morphology of fines, thus, the average fiber length and diameter is not considering
298 fines length and diameter. The presence of such fines may be beneficial for the fibrillation process
299 during high-pressure homogenization. Indeed, the 150 min-treated pulp did not exhibit any
300 clogging during fibrillation, contrarily to lower processing times. The changes on fiber
301 morphology, together with the generation of fines, also had a significant effect over the SSA and
302 the CD. SSA increased from 2.87 to 16.01 m²/g and CD, from 56.3 to 137.6 $\mu\text{eq/g}$. In previous
303 works, authors already reported that CD can be a good indicator of the SSA [46,64]. In the case
304 of BTMP, this correlation was confirmed, as reflected in Fig. 1.

305 [FIGURE 1 ABOUT HERE]

306 For all the above, the treatment time in the Valley beater was set at 150 min, considering that no
307 clogging was observed during high-pressure homogenization and that both SSA and CD, and the
308 morphological characteristics were, in principle, significantly better for LCMNF production than
309 the rest of treated pulps at shorter periods.

310 3.3 Production and characterization of the LCMNF

311 The selected pulp was passed through the high-pressure homogenizer at different numbers of
312 passes and pressure, according to the conditions specified in the previous section. Table 5 shows
313 the yield of nanofibrillation, transmittance at 600 nm wavelength ($T_{600\text{nm}}$), WRV, CD and SSA of
314 the different LCMNF. SSA was obtained by means of Congo red (SSA_{CR}) and polyDADMAC
315 adsorption ($\text{SSA}_{\text{p+}}$).

316 [TABLE 5 ABOUT HERE]

317 As expected, yield of nanofibrillation increased with the number of passes and pressure through
318 the high-pressure homogenizer. LCMNF 1 and LCMNF 2 exhibited a low yield of
319 nanofibrillation, accounting for 4.6 and 11.9 %. These low yields indicate that only a small
320 fraction of nanosized fibers can be obtained by means of passing the suspension through the high-
321 pressure homogenizer at low-moderate pressure (300 – 600 bar). Once the suspension was passed
322 through the pressure chambers at 900 bar, the yield of nanofibrillation increased to 24.1%
323 (LCMNF 3) and, conducting the operation at 900 bar three additional times, this yield was just
324 increased to 28.6 % (LCMNF 4). Indeed, such low yields compared to other suspensions of
325 nanofibrillated cellulose are completely understandable, as neither negatively charged groups are
326 introduced in the cellulose chain (i.e. TEMPO-mediated oxidation) nor specific mechanisms
327 based on enzyme action are occurring (i.e. enzymatic hydrolysis) [65].

328 It is clear that the raw material also has a direct influence on the yield of nanofibrillation. Indeed,
329 in previous works, lignocellulosic micro/nanofibers obtained from chemical pulps usually lead to
330 higher nanofibrillation yields, such is the case of wheat or alkali-treated mechanical pine pulp,
331 and of the same magnitude than other mechanical pulps such as banana leaf residue or *triticale*
332 straw [46,50,66,67].

333 The differences in the yield of nanofibrillation were also observed in the transmittance of the
334 suspensions at 600 nm. Transmittance is often used as an indirect indicator of the nanofibrillation
335 yield, as the higher presence of nanosized fibers in the suspension minimizes light scattering [68].
336 Table 5 reveals that as the intensity in the high-pressure homogenizer was increased,
337 transmittance also experienced an increase. However, the obtained values are far from those that
338 may offer purely nanostructured cellulose, mainly due to a combined phenomenon of low

339 fibrillation degree and the presence of lignin. Thus, it becomes apparent that the obtained LCMNF
340 suspensions contained both nano- and microsized fibrils, as it can be observed in Fig. 2.

341 **[FIGURE 2 ABOUT HERE]**

342 Fig. 2 evidences the presence of both micro and nano fibers in the suspensions. Fig. 2A shows a
343 microfibril with an approximate diameter of 1 μm , whereas nanofibrils at their surface with
344 diameters in the range of 56.2 to 78.9 nm can be clearly seen. Fig. 2B exhibits a similar scenario,
345 though, as the suspensions has been more intensively fibrillated, the diameter of the nanofibers
346 decreased to a range of 21 to 40 nm. The mix of micro and nanofibers also support the low yield
347 and transmittance values.

348 As expected, the SSA also increased with the successive passes through the homogenizer.
349 However, the differences between the SSA obtained by means of Congo Red adsorption and the
350 one obtained through the polyDADMAC adsorption are worthy to mention. SSA_{CR} exhibited
351 values in the range of 117.8 (LCMNF 1) and 150.3 m^2/g (LCMNF 4). On the other hand, the
352 SSA_{p^+} values were limited from 64.7 (LCMNF 1) to 94.4 m^2/g (LCMNF 4). Several methods
353 have been already reported to determine the SSA of micro and nanostructured cellulose, and all
354 of them are based in different mechanisms. Nonetheless, all the methodologies that can be found
355 in the literature are based on indirect methods, as the estimation of SSA from length and diameter
356 can be misleading due to the presence of surface fibrillation and irregular morphology [50,51,69].
357 Depending on the method, especially in those involving adsorption mechanisms, the order of
358 magnitude of the SSA can significantly differ, as it is the case of SSA_{CR} and SSA_{p^+} . Congo Red
359 molecule has a surface area of 1.73 $\text{nm}^2/\text{molecule}$, while in the case of polyDADMAC, surface
360 area accounts for 535.87 $\text{nm}^2/\text{molecule}$. The lower surface area of Congo Red may propitiate its
361 penetration into the LCMNF structure, apart from its diffusion onto fibers surface as dimers,
362 providing a higher value during the measurement of SSA [70,71]. In addition, the molecular
363 weight (Mw) of polyDADMAC may also have an effect on the determination of SSA, as it has
364 been previously reported. Briefly, low-Mw polyDADMAC (7.5 – 15 kDa) may result in high
365 detected charge due to polymer penetration into the fiber structure, obtaining the fiber total
366 charge. On the other hand, high-Mw poly-DADMAC (> 100 kDa) leads to lower detected charge,
367 as it is only adsorbed on fiber surface [72].

368 As in the case of the mechanically refined pulps, as the SSA of LCMNF increased, a noticeable
369 enhancement of the CD was also observed. The CD increased from 179 to 240 $\mu\text{eq}/\text{g}$ for LCMNF
370 1 and LCMNF 4, respectively. Indeed, the increase on the CD evolved linearly with the SSA as
371 in the case of mechanically refined BTMP. This linear evolution can be observed in Fig. 3A.

372 **[FIGURE 3 ABOUT HERE]**

373 WRV also experienced a great enhancement as the mechanically refined BTMP was gradually
374 passed through the high-pressure homogenizer. This increase on the WRV mainly comes from
375 the increase on the SSA and, thus, the extent of fibrillation. However, other effects may be
376 occurring during high-pressure homogenization, such as lignin release from the microfibrils due
377 to the high shear forces [73]. The WRV increased from 1.5 to 3.1 g/g , corresponding to the
378 LCMNF 1 and LCMNF 4, respectively. Several authors have reported the excellent capacity of
379 nanostructured cellulose to bond water, even to form water-based gels at low solid content. The
380 obtained WRV is lower than values reported in the literature, mainly due to a combined effect
381 between the relatively high lignin content and the lower fibrillation degree [49]. The evolution of
382 the WRV with the CD did not respond to a linear regression, as reflected in Fig. 3B. In principle,
383 considering that WRV has been reported to be a reliable measure to characterize the extent of
384 fibrillation of micro and nanofibrils and, in addition, that SSA evolved linearly with CD, one may
385 expect a linear tendency between WRV and CD [74]. Nonetheless, the evolution of WRV
386 responded to a second order polynomial equation, indicating that an additional effect to the
387 enhancement of the fibrillation was occurring. This was corroborated in Figure 3C, where the
388 evolution of WRV as SSA increased is reflected. This additional effect may be a slight increase
389 of the hydrophilicity of the LCMNF as they were passed through the high-pressure homogenizer.
390 Jonoobi et al., (2015) [75] reported that successive passes through the homogenizer could promote
391 the removal of amorphous regions and, thus, increase the crystallinity of the lignocellulosic
392 suspension. In addition, as mentioned above, Qua et al., (2011) [73] already noticed lignin release
393 from the LCMNF suspension due to the shear forces inside the pressure chambers of the
394 equipment. Another plausible explanation is the decomposition of lignin-derived compounds
395 during the high-pressure homogenization process forming low-Mw and water-soluble compounds
396 [76]. Overall, the chemical composition of LCMNF may experience some changes during the
397 high-pressure homogenization process, either due to the release of surface lignin, decomposition
398 of lignin-derived compounds or even the removal of amorphous regions, including hemicellulose.

399 Aiming at glimpsing the effect of high-pressure homogenization in the chemical structure of
400 LCMNF, the DP, Klason lignin and the crystallinity index was determined for each LCMNF.
401 (Table 6). XRD curves for the determination of the crystallinity index are shown in Fig. 4.

402 **[TABLE 6 ABOUT HERE]**

403 **[FIGURE 4 ABOUT HERE]**

404 The determination of Klason lignin revealed that, as previously discussed, there was some lignin
405 removal during high-pressure homogenization. Indeed, a decrease of about 3 wt.% in the lignin
406 content of the LCMNF was observed (comparing LCMNF 1 and LCMNF 4), together with a great
407 reduction of the DP and a slight increase of the crystallinity index. The highest reduction in the

1 lignin content was observed the first time that suspensions were processed at 900 bar, where
2 409 shearing was significantly more intensive than at lower processing pressures. This decrease on
3 410 the lignin content was also observed in the increase on the crystallinity index, where the highest
4 411 change was also observed when suspensions were processed at the maximum pressure for the first
5 412 time. This higher crystallinity, thus, can be attributed to the loss of lignin during high-pressure
6 413 homogenization. The increase on crystallinity may decrease the hydrophilicity of the LCMNF
7 414 and one could lower WRV. However, the obtained results clearly show that the removal of lignin
8 415 had a greater effect on WRV than the increase of crystallinity.

9 416 As observed before, the CD is highly associated with the nanofibrillation yield and SSA. In
10 417 addition, the difference between the CD and CC can be used to quantify the number of hydroxyls
11 418 available at the fiber surface. Such value can be related to the hydrogen bonding ability and thus
12 419 to the strengthening potential of the nanofibers. The CD can also be useful to attempt different
13 420 chemical modifications on the nanofibers, including esterification, etherification, oxidation,
14 421 silylation, polymer grafting, and others, for various end uses [77]. From the obtained results, CD
15 422 may be used as monitoring parameter for the fibrillation process of LCMNF, though, it presents
16 423 some limitations that should be considered.

17 424 3.4 Limitations of cationic demand as monitoring parameter of fibrillation and 18 425 perspectives

19 426 CD is strongly affected by the surface charge, which may be induced by the introduction of
20 427 functional groups into cellulose structure. A clear example is the TEMPO-mediated oxidation
21 428 process, where highly negatively charged groups (COO^-) are introduced by means of the oxidation
22 429 of the primary alcohol in the C6 of the cellulose chain [11]. Another example could be those
23 430 cellulose nanofibers obtained by means of cationization processes, which are based on the
24 431 introduction of quaternary ammonium groups [78,79]. In addition to this, the chemical
25 432 composition of the starting material may also affect the CD of the micro and nanofibers. Thus,
26 433 the use of CD as monitoring parameter is restricted to processes where the rest of the conditions
27 434 are controlled, and the different correlations may apply to such conditions. To the best of our
28 435 knowledge, the monitoring of the production processes of micro and nanofibers must encompass
29 436 the combination of different parameters integrated in robust models that allow real-time
30 437 characterization, which is something that still needs further research, to diminish the uncertainty
31 438 during production processes. To the authors, such integrative and robust models should integrate
32 439 variables from the raw material, the pretreatment stage and the fibrillation itself, something that
33 440 is still missing and that would promote the full deployment of micro and nanocellulose production
34 441 at large scale.

442 **4 Conclusions**

1
2 443 In this work, LCMNF were prepared by means of mechanical methods, combining mechanical
3
4 444 refining and high-pressure homogenization. It was found that fiber length plays a critical role on
5
6 445 the aptitude of the fibers to be processed by means of high-pressure homogenization, requiring a
7
8 446 treatment in the Valley beater of 150 min in order to shorten the fibers from 1,178 to 682 μm ,
9
10 447 apart from increasing the fines content. From the study at different homogenization intensities, it
11
12 448 can be concluded that the high shearing inside the pressure chambers have a positive effect on
13
14 449 nanofibrillation, especially at operating pressures above 900 bar, where significant effect can be
15
16 450 observed in the different parameters, including nanofibrillation yield, specific surface area,
17
18 451 cationic demand and water retention value, among others. It was found that the high-pressure
19
20 452 homogenization processes affect the lignin content of the fibers and their crystallinity, as the
21
22 453 Klason lignin content decreased from 24.3 to 21.0 wt.% and the crystallinity increased from 70.6
23
24 454 to 75.7%. This was found to have a significant effect over the water retention value of the LCMNF
25
26 455 and limiting the use of this parameter to monitor the extent of fibrillation of the samples.
27
28 456 Contrarily, it was found that cationic demand is a good indicator of the fibrillation of the LCMNF,
29
30 457 as the rest of the parameters evolved linearly at increasing cationic demands. Overall, it can be
31
32 458 concluded that high yield pulps can be useful for LCMNF if they are properly treated and, in
33
34 459 addition, that cationic demand is a suitable parameter to monitor the fibrillation process,
35
36 460 especially in nanostructured cellulose which has not been obtained by means of chemical
37
38 461 methods.

462 **Acknowledgements**

39 463 Authors wish to acknowledge the financial support of the Spanish Economy and Competitiveness
40
41 464 Ministry to the Project NANOPROSOST, Reference CTQ2017-85654.

465 **References**

- 42
43 466 [1] A. Isogai, Emerging Nanocellulose Technologies: Recent Developments, *Adv. Mater.*
44
45 467 (2020) 2000630. <https://doi.org/10.1002/adma.202000630>.
46
47 468 [2] T. Lindström, C. Aulin, A. Naderi, M. Ankerfors, Microfibrillated Cellulose, in: *Encycl.*
48
49 469 *Polym. Sci. Technol.*, John Wiley & Sons, Inc., Hoboken, NJ, USA, 2014: pp. 1–34.
50
51 470 <https://doi.org/10.1002/0471440264.pst614>.
52
53 471 [3] I. Siró, D. Plackett, Microfibrillated cellulose and new nanocomposite materials: A
54
55 472 review, *Cellulose*. 17 (2010) 459–494. <https://doi.org/10.1007/s10570-010-9405-y>.
56
57 473 [4] J.H. Kim, B.S. Shim, H.S. Kim, Y.J. Lee, S.K. Min, D. Jang, Z. Abas, J. Kim, Review of
58
59 474 nanocellulose for sustainable future materials, *Int. J. Precis. Eng. Manuf. - Green*
60
61 475 *Technol.* 2 (2015) 197–213. <https://doi.org/10.1007/s40684-015-0024-9>.
62
63 476 [5] C. Ruiz-Palomero, M.L. Soriano, M. Valcárcel, Nanocellulose as analyte and analytical

- 477 tool: Opportunities and challenges, *TrAC - Trends Anal. Chem.* 87 (2017) 1–18.
478 <https://doi.org/10.1016/j.trac.2016.11.007>.
- 479 [6] K. Keça, C.M. Chaléat, N. Amiralian, W. Batchelor, L. Grøndahl, D.J. Martin,
480 Evaluation of properties and specific energy consumption of spinifex-derived
481 lignocellulose fibers produced using different mechanical processes, *Cellulose*. 26
482 (2019) 6555–6569. <https://doi.org/10.1007/s10570-019-02567-x>.
- 483 [7] M. Jawaid, S. Boufi, A. Khalil, *Cellulose-reinforced nanofibre composites : production,*
484 *properties and applications*, 2017.
- 485 [8] J. Miller, *Nanocellulose: Market perspectives*, *Tappi J.* 18 (2019) 313–316.
- 486 [9] M. Delgado-Aguilar, I. González, Q. Tarres, M. Alcalà, M.A. Pelach, P. Mutje,
487 *Approaching a Low-Cost Production of Cellulose Nanofibers for Papermaking*
488 *Applications*, *BioResources*. 10 (2015) 5345–5355.
- 489 [10] A. Serra, I. González, H. Oliver-Ortega, Q. Tarrès, M. Delgado-Aguilar, P. Mutjé,
490 *Reducing the Amount of Catalyst in TEMPO-Oxidized Cellulose Nanofibers: Effect on*
491 *Properties and Cost*, *Polymers (Basel)*. 9 (2017) 557.
492 <https://doi.org/10.3390/polym9110557>.
- 493 [11] A. Isogai, T. Saito, H. Fukuzumi, *TEMPO-oxidized cellulose nanofibers*, *Nanoscale*. 3
494 (2011) 71–85. <https://doi.org/10.1039/c0nr00583e>.
- 495 [12] T. Saito, S. Kimura, Y. Nishiyama, A. Isogai, *Cellulose Nanofibers Prepared by*
496 *TEMPO-Mediated Oxidation of Native Cellulose*, *Biomacromolecules*. 8 (2007) 2485–
497 2491. <https://doi.org/10.1021/bm0703970>.
- 498 [13] R. Singla, A. Guliani, A. Kumari, S.K. Yadav, *Nanocellulose and nanocomposites*, in:
499 *Nanoscale Mater. Target. Drug Deliv. Theragnosis Tissue Regen.*, Springer Singapore,
500 2016: pp. 103–125. https://doi.org/10.1007/978-981-10-0818-4_5.
- 501 [14] C.I.K. Diop, M. Tajvidi, M.A. Bilodeau, D.W. Bousfield, J.F. Hunt, *Isolation of*
502 *lignocellulose nanofibrils (LCNF) and application as adhesive replacement in wood*
503 *composites: example of fiberboard*, *Cellulose*. 24 (2017) 3037–3050.
504 <https://doi.org/10.1007/s10570-017-1320-z>.
- 505 [15] L. Kuutti, H. Pajari, S. Rovio, J. Kokkonen, M. Nuopponen, *Chemical recovery in*
506 *TEMPO oxidation*, *BioResources*. 11 (2016) 6050–6061.
- 507 [16] M. Pedersen, A.S. Meyer, *Lignocellulose pretreatment severity - relating pH to*
508 *biomatrix opening*, *N. Biotechnol.* 27 (2010) 739–750.
509 <https://doi.org/10.1016/j.nbt.2010.05.003>.
- 510 [17] R.S.A. Ribeiro, B.C. Pohlmann, V. Calado, N. Bojorge, N. Pereira, *Production of*
511 *nanocellulose by enzymatic hydrolysis: Trends and challenges*, *Eng. Life Sci.* 19 (2019)
512 279–291. <https://doi.org/10.1002/elsc.201800158>.
- 513 [18] A. Balea, E. Fuente, M.C. Monte, N. Merayo, C. Campano, C. Negro, A. Blanco,

- 1
2
3
4
5
6
7
8
9
10
11
12
13
14
15
16
17
18
19
20
21
22
23
24
25
26
27
28
29
30
31
32
33
34
35
36
37
38
39
40
41
42
43
44
45
46
47
48
49
50
51
52
53
54
55
56
57
58
59
60
61
62
63
64
65
- 514 Industrial Application of Nanocelluloses in Papermaking: A Review of Challenges,
515 Technical Solutions, and Market Perspectives, *Molecules*. 25 (2020) 526.
516 <https://doi.org/10.3390/molecules25030526>.
- [19] 517 R.H. Newman, Carbon-13 NMR evidence for cocrystallization of cellulose as a
518 mechanism for hornification of bleached kraft pulp, *Cellulose*. 11 (2004) 45–52.
519 <https://doi.org/10.1023/B:CELL.0000014768.28924.0c>.
- [20] 520 K.L. Spence, R.A. Venditti, O.J. Rojas, Y. Habibi, J.J. Pawlak, The effect of chemical
521 composition on microfibrillar cellulose films from wood pulps: Water interactions and
522 physical properties for packaging applications, *Cellulose*. 17 (2010) 835–848.
523 <https://doi.org/10.1007/s10570-010-9424-8>.
- [21] 524 M. Visanko, J.A. Sirviö, P. Piltonen, R. Sliz, H. Liimatainen, M. Illikainen, Mechanical
525 fabrication of high-strength and redispersible wood nanofibers from unbleached
526 groundwood pulp, *Cellulose*. 24 (2017) 4173–4187. [https://doi.org/10.1007/s10570-017-](https://doi.org/10.1007/s10570-017-1406-7)
527 [1406-7](https://doi.org/10.1007/s10570-017-1406-7).
- [22] 528 M. El Bakkari, V. Bindiganavile, J. Goncalves, Y. Boluk, Preparation of cellulose
529 nanofibers by TEMPO-oxidation of bleached chemi-thermomechanical pulp for cement
530 applications, *Carbohydr. Polym.* 203 (2019) 238–245.
531 <https://doi.org/10.1016/j.carbpol.2018.09.036>.
- [23] 532 E. Rojo, M.S. Peresin, W.W. Sampson, I.C. Hoeger, J. Vartiainen, J. Laine, O.J. Rojas,
533 Comprehensive elucidation of the effect of residual lignin on the physical, barrier,
534 mechanical and surface properties of nanocellulose films, *Green Chem.* 17 (2015) 1853–
535 1866. <https://doi.org/10.1039/c4gc02398f>.
- [24] 536 M. Sánchez-Gutiérrez, E. Espinosa, I. Bascón-Villegas, F. Pérez-Rodríguez, E. Carrasco,
537 A. Rodríguez, Production of Cellulose Nanofibers from Olive Tree Harvest—A Residue
538 with Wide Applications, *Agronomy*. 10 (2020) 696.
539 <https://doi.org/10.3390/agronomy10050696>.
- [25] 540 S.H. Osong, Mechanical Pulp Based Nano-ligno-cellulose Production, Characterization
541 and their Effect on Paper Properties, (2014) 57.
- [26] 542 Y. Wen, Z. Yuan, X. Liu, J. Qu, S. Yang, A. Wang, C. Wang, B. Wei, J. Xu, Y. Ni,
543 Preparation and Characterization of Lignin-Containing Cellulose Nanofibril from Poplar
544 High-Yield Pulp via TEMPO-Mediated Oxidation and Homogenization, *ACS Sustain.*
545 *Chem. Eng.* 7 (2019) 6131–6139. <https://doi.org/10.1021/acssuschemeng.8b06355>.
- [27] 546 B. Li, H. Li, Q. Zha, R. Bandekar, A. Alsaggaf, Y. Ni, Review: Effects of wood quality
547 and refining process on TMP pulp and paper quality, *BioResources*. 6 (2011) 3569–
548 3584.
- [28] 549 S.H. Osong, S. Norgren, P. Engstrand, Paper strength improvement by inclusion of
550 nano-ligno-cellulose to Chemi-thermomechanical pulp, *Nord. Pulp Pap. Res. J.* 29

- 551 (2014) 309–316. <https://doi.org/10.3183/npprj-2014-29-02-p309-316>.
- 1 552 [29] M. Henriksson, G. Henriksson, L.A. Berglund, T. Lindström, T. Lindstrom, T. Lindstro,
2
3 553 An environmentally friendly method for enzyme-assisted preparation of microfibrillated
4
5 554 cellulose (MFC) nanofibers, *Eur. Polym. J.* 43 (2007) 3434–3441.
- 6 555 [30] K.L. Spence, R.A. Venditti, O.J. Rojas, Y. Habibi, J.J. Pawlak, A comparative study of
7
8 556 energy consumption and physical properties of microfibrillated cellulose produced by
9
10 557 different processing methods, *Cellulose*. 18 (2011) 1097–1111.
11
12 558 <https://doi.org/10.1007/s10570-011-9533-z>.
- 13 559 [31] A.F. Turbak, F.W. Snyder, K.R. Sandberg, Microfibrillated cellulose, a new cellulose
14
15 560 product: properties, uses, and commercial potential, *J. Appl. Polym. Sci.* 37 (1983).
- 16 561 [32] E. Espinosa, F. Rol, J. Bras, A. Rodríguez, Use of multi-factorial analysis to determine
17
18 562 the quality of cellulose nanofibers: effect of nanofibrillation treatment and residual lignin
19
20 563 content, *Cellulose*. (2020) 1–17. <https://doi.org/10.1007/s10570-020-03136-3>.
- 21 564 [33] J. Desmaisons, E. Boutonnet, M. Rueff, A. Dufresne, J. Bras, A new quality index for
22
23 565 benchmarking of different cellulose nanofibrils, *Carbohydr. Polym.* 174 (2017) 318–329.
24
25 566 <https://doi.org/10.1016/j.carbpol.2017.06.032>.
- 26 567 [34] A. Balea, J.L. Sanchez-Salvador, M.C. Monte, N. Merayo, C. Negro, A. Blanco, In situ
27
28 568 production and application of cellulose nanofibers to improve recycled paper production,
29
30 569 *Molecules*. 24 (2019). <https://doi.org/10.3390/molecules24091800>.
- 31 570 [35] L.A. Berglund, T. Peijs, Cellulose Biocomposites—From Bulk Moldings to
32
33 571 Nanostructured Systems, *MRS Bull.* 35 (2010) 201–207.
34
35 572 <https://doi.org/10.1557/mrs2010.652>.
- 36 573 [36] A. Dufresne, Cellulose nanomaterials as green nanoreinforcements for polymer
37
38 574 nanocomposites, *Philos. Trans. R. Soc. A Math. Phys. Eng. Sci.* 376 (2018).
39
40 575 <https://doi.org/10.1098/rsta.2017.0040>.
- 41 576 [37] D. Klemm, F. Kramer, S. Moritz, T. Lindström, M. Ankerfors, D. Gray, A. Dorris,
42
43 577 Nanocelluloses: A New Family of Nature-Based Materials, *Angew. Chemie Int. Ed.* 50
44
45 578 (2011) 5438–5466. <https://doi.org/10.1002/anie.201001273>.
- 46 579 [38] R.J. Moon, A. Martini, J. Nairn, J. Simonsen, J. Youngblood, Cellulose nanomaterials
47
48 580 review: Structure, properties and nanocomposites, *Chem. Soc. Rev.* 40 (2011) 3941–
49
50 581 3994. <https://doi.org/10.1039/c0cs00108b>.
- 51 582 [39] Y. Nishiyama, Structure and properties of the cellulose microfibril, *J. Wood Sci.* 55
52
53 583 (2009) 241–249. <https://doi.org/10.1007/s10086-009-1029-1>.
- 54 584 [40] A. Winter, L. Andorfer, S. Herzele, T. Zimmermann, B. Saake, M. Edler, T. Griesser, J.
55
56 585 Konnerth, W. Gindl-Altmutter, Reduced polarity and improved dispersion of
57
58 586 microfibrillated cellulose in poly(lactic-acid) provided by residual lignin and
59
60 587 hemicellulose, *J. Mater. Sci.* 52 (2017) 60–72. <https://doi.org/10.1007/s10853-016-0439->

- 588 x.
- 1 589 [41] J. Ojala, J.A. Sirviö, H. Liimatainen, Nanoparticle emulsifiers based on bifunctionalized
2 cellulose nanocrystals as marine diesel oil-water emulsion stabilizers, *Chem. Eng. J.* 288
3 (2016) 312–320. <https://doi.org/10.1016/j.cej.2015.10.113>.
4
5 591
- 6 592 [42] D. Theng, G. Arbat, M. Delgado-Aguilar, F. Vilaseca, B. Ngo, P. Mutjé, All-
7 lignocellulosic fiberboard from corn biomass and cellulose nanofibers, *Ind. Crops Prod.*
8 76 (2015) 166–173. <https://doi.org/10.1016/j.indcrop.2015.06.046>.
9
10 594
- 11 595 [43] D. Kai, W. Ren, L. Tian, P.L. Chee, Y. Liu, S. Ramakrishna, X.J. Loh, Engineering
12 Poly(lactide)–Lignin Nanofibers with Antioxidant Activity for Biomedical Application,
13 *ACS Sustain. Chem. Eng.* 4 (2016) 5268–5276.
14
15 597
16 598 <https://doi.org/10.1021/acssuschemeng.6b00478>.
17
- 18 599 [44] F. Reesi, M. Minaiyan, A. Taheri, A novel lignin-based nanofibrous dressing containing
19 arginine for wound-healing applications, *Drug Deliv. Transl. Res.* 8 (2018) 111–122.
20
21 600
22 601 <https://doi.org/10.1007/s13346-017-0441-0>.
- 23 602 [45] Future Markets Inc., The global market for cellulose nanofibers, 2020.
24
25 603 www.futuremarketsinc.com.
- 26 604 [46] Q. Tarrés, N.V. Ehman, M.E. Vallejos, M.C. Area, M. Delgado-Aguilar, P. Mutjé,
27 Lignocellulosic nanofibers from triticale straw: The influence of hemicelluloses and
28 lignin in their production and properties, *Carbohydr. Polym.* 163 (2017) 20–27.
29
30 606
31 607 <https://doi.org/10.1016/j.carbpol.2017.01.017>.
- 32
33 608 [47] A. Naderi, T. Lindström, J. Sundström, Repeated homogenization, a route for decreasing
34 the energy consumption in the manufacturing process of carboxymethylated
35 nanofibrillated cellulose?, *Cellulose.* 22 (2015) 1147–1157.
36
37 610
38 611 <https://doi.org/10.1007/s10570-015-0576-4>.
- 39
40 612 [48] D. da Silva Perez, S. Montanari, M.R. Vignon, TEMPO-mediated oxidation of cellulose
41 III, *Biomacromolecules.* 4 (2003) 1417–1425. <https://doi.org/10.1021/bm034144s>.
42
43 614 [49] J. Patiño-Masó, F. Serra-Parareda, Q. Tarrés, P. Mutjé, F.X. Espinach, M. Delgado-
44 Aguilar, TEMPO-Oxidized Cellulose Nanofibers: A Potential Bio-Based Superabsorbent
45 for Diaper Production, *Nanomaterials.* 9 (2019) 1271.
46
47 616
48 617 <https://doi.org/10.3390/nano9091271>.
- 49
50 618 [50] E. Espinosa, Q. Tarrés, M. Delgado-Aguilar, I. González, P. Mutjé, A. Rodríguez,
51 Suitability of wheat straw semichemical pulp for the fabrication of lignocellulosic
52 nanofibres and their application to papermaking slurries, *Cellulose.* 23 (2016) 837–852.
53
54 620
55 621 <https://doi.org/10.1007/s10570-015-0807-8>.
- 56
57 622 [51] A. Ferrer, E. Quintana, I. Filpponen, I. Solala, T. Vidal, A. Rodríguez, J. Laine, O.J.
58 Rojas, Effect of residual lignin and heteropolysaccharides in nanofibrillar cellulose and
59 nanopaper from wood fibers, *Cellulose.* 19 (2012) 2179–2193.
60
61 624

- 625 <https://doi.org/10.1007/s10570-012-9788-z>.
- 1 626 [52] L. Segal, J.J. Creely, A.E. Martin, C.M. Conrad, An Empirical Method for Estimating
2 the Degree of Crystallinity of Native Cellulose Using the X-Ray Diffractometer, *Text.*
3 *Res. J.* 29 (1959) 786–794. <https://doi.org/10.1177/004051755902901003>.
- 4 627
5 628
6 629 [53] A. Tutus, S. Ates, I. Deniz, Pulp and paper production from Spruce wood with kraft and
7 modified kraft methods, *African J. Biotechnol.* 9 (2010) 1648–1654.
- 8 630
9 631 [54] E.L. Hult, P.T. Larsson, T. Iversen, Comparative CP/MAS ¹³C-NMR study of cellulose
10 structure in spruce wood and kraft pulp, *Cellulose.* 7 (2000) 35–55.
11
12 632
13 633 <https://doi.org/10.1023/A:1009236932134>.
- 14 634 [55] Z. Wang, S. Winestrand, T. Gillgren, L.J. Jönsson, Chemical and structural factors
15 influencing enzymatic saccharification of wood from aspen, birch and spruce, *Biomass*
16 *and Bioenergy.* 109 (2018) 125–134. <https://doi.org/10.1016/j.biombioe.2017.12.020>.
- 17 635
18 636 [56] M. Jonoobi, A.P. Mathew, K. Oksman, Natural Resources and Residues for Production
19 of Bionanomaterials, in: 2014: pp. 19–33. https://doi.org/10.1142/9789814566469_0003.
- 20 637
21 638 [57] A. Chaker, S. Alila, P. Mutjé, M.R. Vilar, S. Boufi, Key role of the hemicellulose
22 content and the cell morphology on the nanofibrillation effectiveness of cellulose pulps,
23 *Cellulose.* 20 (2013) 2863–2875. <https://doi.org/10.1007/s10570-013-0036-y>.
- 24 639
25 640 [58] M. Sánchez-Gutiérrez, E. Espinosa, I. Bascón-Villegas, F. Pérez-Rodríguez, E. Carrasco,
26 A. Rodríguez, Production of Cellulose Nanofibers from Olive Tree Harvest—A Residue
27 with Wide Applications, *Agronomy.* 10 (2020) 696.
28
29 641
30 642 <https://doi.org/10.3390/agronomy10050696>.
- 31 643
32 644 [59] L. Berglund, M. Noël, Y. Aitomäki, T. Öman, K. Oksman, Production potential of
33 cellulose nanofibers from industrial residues: Efficiency and nanofiber characteristics,
34 *Ind. Crops Prod.* 92 (2016) 84–92. <https://doi.org/10.1016/j.indcrop.2016.08.003>.
- 35 645
36 646 [60] S. Mansouri, R. Khiari, N. Bendouissa, S. Saadallah, F. Mhenni, E. Mauret, Chemical
37 composition and pulp characterization of Tunisian vine stems, *Ind. Crops Prod.* 36
38 (2012) 22–27. <https://doi.org/10.1016/j.indcrop.2011.07.036>.
- 39 647
40 648 [61] S.P. Mishra, Bleaching of cellulosic paper fibres with ozone-effect on the fibre
41 properties, Institut Polytechnique de Grenoble, France, 2010.
- 42 649
43 650 [62] M.E. Vallejos, F.E. Felissia, M.C. Area, N.V. Ehman, Q. Tarrés, P. Mutjé,
44 Nanofibrillated cellulose (CNF) from eucalyptus sawdust as a dry strength agent of
45 unrefined eucalyptus handsheets, *Carbohydr. Polym.* 139 (2016) 99–105.
46
47 651
48 652 <https://doi.org/10.1016/j.carbpol.2015.12.004>.
- 49 653
50 654 [63] M.A. Arsène, K. Bilba, C. Onésippe, Treatments for viable utilization of vegetable fibers
51 in inorganic-based composites, in: *Sustain. Nonconv. Constr. Mater. Using Inorg. Bond.*
52 *Fiber Compos.*, Elsevier Inc., 2017: pp. 70–123. [https://doi.org/10.1016/B978-0-08-](https://doi.org/10.1016/B978-0-08-102001-2.00004-8)
53
54 655
55 656
56 657
57 658
58 659
59 660
60 661
61
62
63
64
65

1
2
3
4
5
6
7
8
9
10
11
12
13
14
15
16
17
18
19
20
21
22
23
24
25
26
27
28
29
30
31
32
33
34
35
36
37
38
39
40
41
42
43
44
45
46
47
48
49
50
51
52
53
54
55
56
57
58
59
60
61
62
63
64
65

662 [64] I. Filipova, F. Serra, Q. Tarrés, P. Mutjé, M. Delgado-Aguilar, Oxidative treatments for
663 cellulose nanofibers production: a comparative study between TEMPO-mediated and
664 ammonium persulfate oxidation, *Cellulose*. (2020) 1–18.

665 [65] Q. Tarrés, S. Boufi, P. Mutjé, M. Delgado-Aguilar, Enzymatically hydrolyzed and
666 TEMPO-oxidized cellulose nanofibers for the production of nanopapers: morphological,
667 optical, thermal and mechanical properties, *Cellulose*. 24 (2017) 3943–3954.
668 <https://doi.org/10.1007/s10570-017-1394-7>.

669 [66] M. Delgado-Aguilar, I. González, Q. Tarrés, M.À. Pèlach, M. Alcalà, P. Mutjé, The key
670 role of lignin in the production of low-cost lignocellulosic nanofibres for papermaking
671 applications, *Ind. Crops Prod*. 86 (2016) 295–300.
672 <https://doi.org/10.1016/j.indcrop.2016.04.010>.

673 [67] Q. Tarrés, E. Espinosa, J. Domínguez-Robles, A. Rodríguez, P. Mutjé, M. Delgado-
674 Aguilar, The suitability of banana leaf residue as raw material for the production of high
675 lignin content micro/nano fibers: From residue to value-added products, *Ind. Crops Prod*.
676 99 (2017) 27–33. <https://doi.org/10.1016/j.indcrop.2017.01.021>.

677 [68] L. Hu, G. Zheng, J. Yao, N. Liu, B. Weil, M. Eskilsson, E. Karabulut, Z. Ruan, S. Fan,
678 J.T. Bloking, M.D. McGehee, L. Wågberg, Y. Cui, Transparent and conductive paper
679 from nanocellulose fibers, *Energy Environ. Sci*. 6 (2013) 513–518.
680 <https://doi.org/10.1039/c2ee23635d>.

681 [69] X. Wang, Y. Zhang, H. Jiang, Y. Song, Z. Zhou, H. Zhao, Fabrication and
682 characterization of nano-cellulose aerogels via supercritical CO₂ drying technology,
683 *Mater. Lett*. 183 (2016) 179–182. <https://doi.org/10.1016/j.matlet.2016.07.081>.

684 [70] M.K. Inglesby, S.H. Zeronian, Direct dyes as molecular sensors to characterize cellulose
685 substrates, *Cellulose*. 9 (2002) 19–29. <https://doi.org/10.1023/A:1015840111614>.

686 [71] H. Bian, Y. Gao, R. Wang, Z. Liu, W. Wu, H. Dai, Contribution of lignin to the surface
687 structure and physical performance of cellulose nanofibrils film, *Cellulose*. 25 (2018)
688 1309–1318. <https://doi.org/10.1007/s10570-018-1658-x>.

689 [72] H. Zhang, C. Zhao, Z. Li, J. Li, The fiber charge measurement depending on the poly-
690 DADMAC accessibility to cellulose fibers, *Cellulose*. 23 (2016) 163–173.

691 [73] E.H. Qua, P.R. Hornsby, H.S.S. Sharma, G. Lyons, Preparation and characterisation of
692 cellulose nanofibres, *J. Mater. Sci*. 46 (2011) 6029–6045.
693 <https://doi.org/10.1007/s10853-011-5565-x>.

694 [74] F. Gu, W. Wang, Z. Cai, F. Xue, Y. Jin, J.Y. Zhu, Water retention value for
695 characterizing fibrillation degree of cellulosic fibers at micro and nanometer scales,
696 *Cellulose*. 25 (2018) 2861–2871. <https://doi.org/10.1007/s10570-018-1765-8>.

697 [75] M. Jonoobi, R. Oladi, Y. Davoudpour, K. Oksman, A. Dufresne, Y. Hamzeh, R.
698 Davoodi, Different preparation methods and properties of nanostructured cellulose from

699 various natural resources and residues: a review, *Cellulose*. 22 (2015) 935–969.

1
2 700 [76] R. He, X.P. Ye, F. Harte, B. English, Effects of high-pressure homogenization on
3 701 physicochemical properties and storage stability of switchgrass bio-oil, *Fuel Process.*
4 702 *Technol.* 90 (2009) 415–421. <https://doi.org/10.1016/j.fuproc.2008.11.003>.

5
6 703 [77] I. Mohammad Tajul, M.M. Alam, M. Zoccola, Review on modification of nanocellulose
7 704 for application in composites, *Int. J. Innov. Res. Sci. Eng. Technol.* 2 (2013) 5444–5451.

8
9 705 [78] H. Yang, T.G. van de Ven, Preparation of hairy cationic nanocrystalline cellulose,
10 706 *Cellulose*. 23 (2016) 1791–1801.

11
12 707 [79] W. Maatar, S. Boufi, Microporous cationic nanofibrillar cellulose aerogel as promising
13 708 adsorbent of acid dyes, *Cellulose2*. 24 (2017) 1001–1015.

14
15
16 709
17
18
19
20
21
22
23
24
25
26
27
28
29
30
31
32
33
34
35
36
37
38
39
40
41
42
43
44
45
46
47
48
49
50
51
52
53
54
55
56
57
58
59
60
61
62
63
64
65

710 **Tables**

711 **Table 1.** Samples and HPH sequence

Sample	Sequence in the HPH n° of passes x pressure (bar)
LCMNF 1	3 x 300
LCMNF 2	3 x 300 + 3 x 600
LCMNF 3	3 x 300 + 3 x 600 + 3 x 900
LCMNF 4	3 x 300 + 3 x 600 + 6 x 900

712

1
2
3
4
5
6
7
8
9
10
11
12
13
14
15
16
17
18
19
20
21
22
23
24
25
26
27
28
29
30
31
32
33
34
35
36
37
38
39
40
41
42
43
44
45
46
47
48
49
50
51
52
53
54
55
56
57
58
59
60
61
62
63
64
65

713 **Table 2.** Chemical composition of the BTMP.

	Cellulose	Hemicellulose	Klason lignin	Extractives	Ashes	Reference
	(wt.%)	(wt.%)	(wt.%)	(wt.%)	(wt.%)	
BTMP	48.35 ± 0.53	25.40 ± 0.31	25.80 ± 0.21	0.25 ± 0.03	0.20 ± 0.05	Present work
UKSP	86.20	11.30	2.23	0.07	0.20	Tutus et al., 2010
BKSP	93.2	6.9	< 0.1	-	-	Hult et al., 2000

714

1
2
3
4
5
6
7
8
9
10
11
12
13
14
15
16
17
18
19
20
21
22
23
24
25
26
27
28
29
30
31
32
33
34
35
36
37
38
39
40
41
42
43
44
45
46
47
48
49
50
51
52
53
54
55
56
57
58
59
60
61
62
63
64
65

715 **Table 3.** Morphology and drainability of BTMP

1	l_w^F (μm)	$1,178 \pm 42$
2	d^F (μm)	29.8 ± 0.2
3	f_{length} (%)	51.9 ± 3.1
4	f_{weight} (%)	12.0 ± 0.9
5	SSA (m^2/g)	2.87 ± 0.12
6	$^{\circ}\text{SR} / \text{CSF}$	$21.5 / 578$

716 Abbreviations: mean fiber length weighted in length (l_w^F), mean fiber diameter (d^F), percentage of fines
 717 weighted in length (f_{length}), percentage of fines in weight (f_{weight}) and specific surface area (SSA)

718 **Table 4.** BTMP characteristics as function of refining time

Valley beater (min)	I_w^F (μm)	d^F (μm)	f_{length} (%)	f_{weight} (%)	DP	SSA (m^2/g)	CD ($\mu\text{eq/g}$)	Aptitude to homogenization
0	$1,178 \pm 42$	29.8 ± 0.2	51.9 ± 1.1	12.0 ± 0.9	$3,250 \pm 93$	2.87 ± 0.12	56.3 ± 1.6	Clogging
50	$1,064 \pm 32$	28.8 ± 0.1	59.0 ± 0.5	24.6 ± 1.9	$3,150 \pm 51$	6.74 ± 0.09	72.4 ± 2.3	Clogging
100	790 ± 51	28.5 ± 0.2	65.2 ± 1.3	31.8 ± 2.2	$2,690 \pm 94$	12.45 ± 0.18	109.5 ± 2.4	Clogging
150	682 ± 29	28.6 ± 0.3	79.5 ± 0.8	40.6 ± 1.3	$2,540 \pm 71$	16.01 ± 0.10	137.6 ± 3.0	Non-clogging

719

1
2
3
4
5
6
7
8
9
10
11
12
13
14
15
16
17
18
19
20
21
22
23
24
25
26
27
28
29
30
31
32
33
34
35
36
37
38
39
40
41
42
43
44
45
46
47
48
49
50
51
52
53
54
55
56
57
58
59
60
61
62
63
64
65

720 **Table 5.** Characterization of the LCMNF

Sample	Yield (%)	T _{600nm} (%)	WRV (g/g)	CD (μeq·g/g)	SSA _{CR} (m ² /g)	SSA _{p+} (m ² /g)
LCMNF 1	4.6 ± 0.3	3.8	1.5 ± 0.1	179 ± 6	117.8	64.7
LCMNF 2	11.9 ± 0.3	8.1	1.8 ± 0.1	205 ± 4	134.4	77.4
LCMNF 3	24.1 ± 0.2	14.5	2.6 ± 0.2	233 ± 2	145.2	91.0
LCMNF 4	28.6 ± 0.4	17.2	3.1 ± 0.1	240 ± 3	150.3	94.4

721

1
2
3
4
5
6
7
8
9
10
11
12
13
14
15
16
17
18
19
20
21
22
23
24
25
26
27
28
29
30
31
32
33
34
35
36
37
38
39
40
41
42
43
44
45
46
47
48
49
50
51
52
53
54
55
56
57
58
59
60
61
62
63
64
65

722 **Table 6.** Characterization of lignocellulosic micro-nano fibers (LCMNF)

Sample	DP (-)	Klason lignin (wt.%)	C.I. (%)
LCMNF 1	755	24.3 ± 0.3	70.6
LCMNF 2	561	23.4 ± 0.1	71.9
LCMNF 3	418	22.1 ± 0.2	75.1
LCMNF 4	367	21.0 ± 0.2	75.7

723 Abbreviations: Degree of polymerization (DP) and crystallinity index (C.I.)

1
2
3
4
5
6
7
8
9
10
11
12
13
14
15
16
17
18
19
20
21
22
23
24
25
26
27
28
29
30
31
32
33
34
35
36
37
38
39
40
41
42
43
44
45
46
47
48
49
50
51
52
53
54
55
56
57
58
59
60
61
62
63
64
65

724 **List of Figures**

- 1
2 725 1. Evolution of SSA and CD at different processing times in the Valley beater.
3
4 726 2. FE-SEM observation of LCMNF 1 (A) and LCMNF 4 (B)
5 727 3. Evolution of the SSA_{CR} (A) and WRV (B) with the CD, and WRV with the SSA_{CR} of
6
7 728 the LCMNF (C).
8
9 729 4. XRD analysis of the LCMNF

10
11
12
13
14
15
16
17
18
19
20
21
22
23
24
25
26
27
28
29
30
31
32
33
34
35
36
37
38
39
40
41
42
43
44
45
46
47
48
49
50
51
52
53
54
55
56
57
58
59
60
61
62
63
64
65

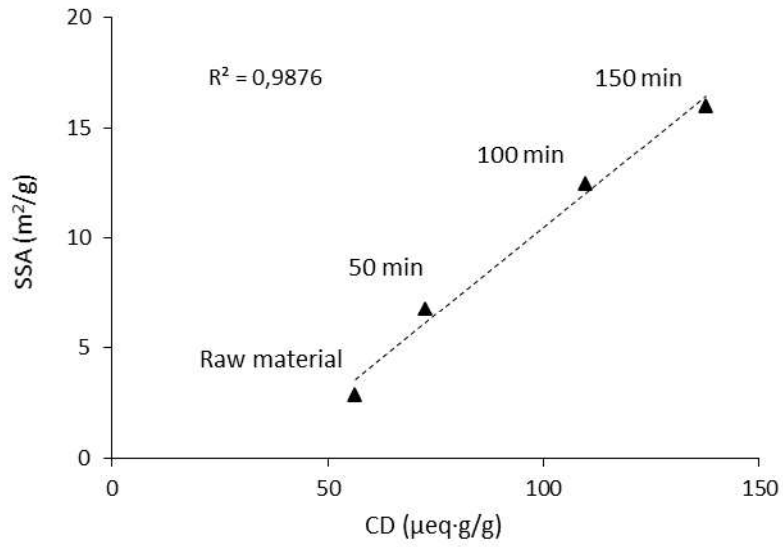
730 **Figures**

731 **Figure 1**

732 - Journal: International Journal of Biological Macromolecules

733 - Author: Ferran Serra-Parareda

734 - Illustration number: 1



735

736 **Figure 1.** Evolution of SSA and CD at different processing times in the Valley beater.

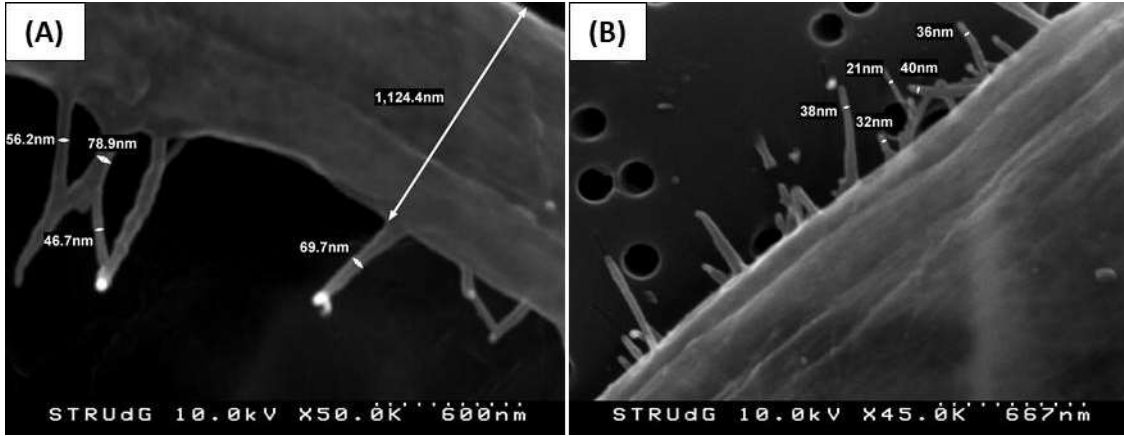
737

738 **Figure 2**

739 - Journal: International Journal of Biological Macromolecules

740 - Author: Ferran Serra-Parareda

741 - Illustration number: 2



742

743 **Figure 2.** FE-SEM observation of LCMNF 1 (A) and LCMNF 4 (B)

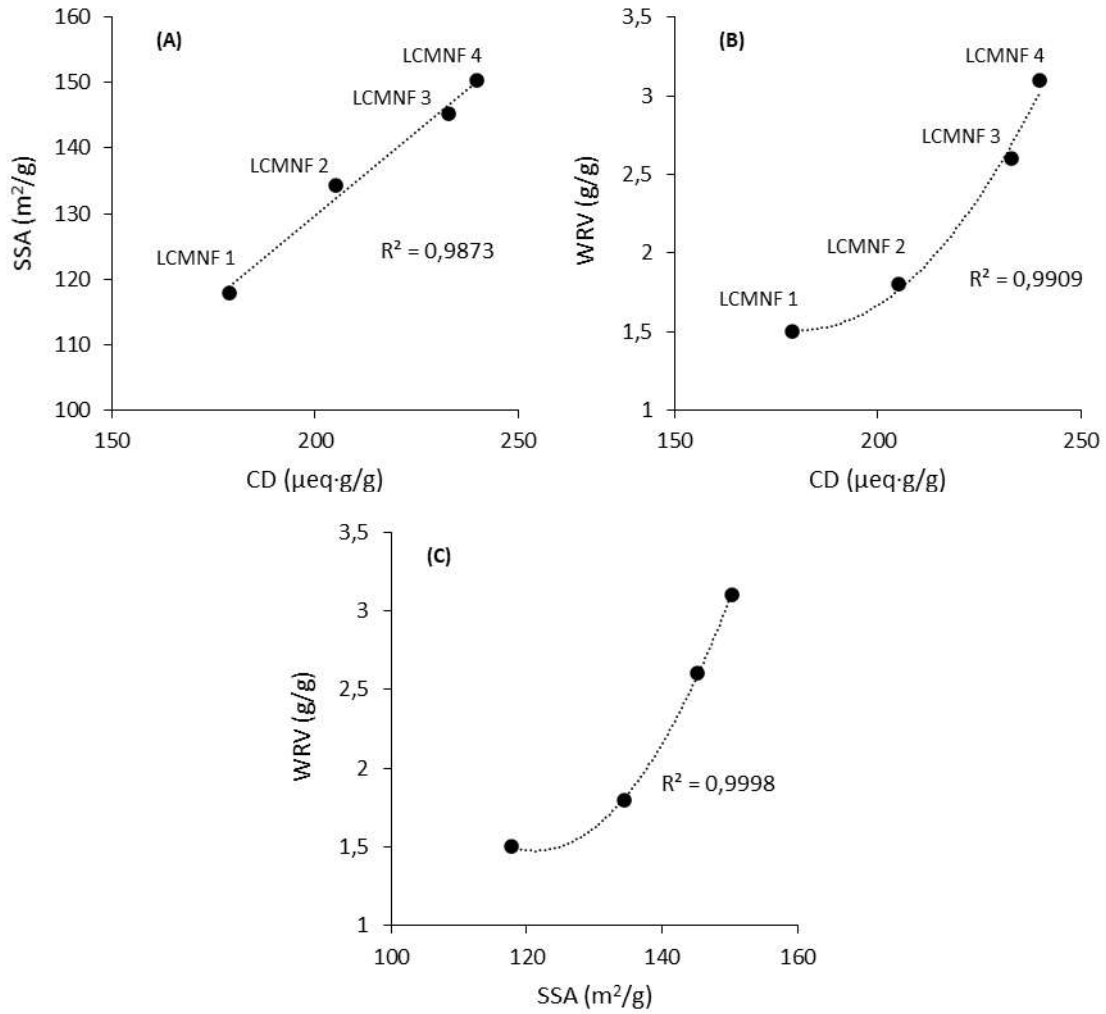
744

745 **Figure 3**

746 - Journal: International Journal of Biological Macromolecules

747 - Author: Ferran Serra-Parareda

748 - Illustration number: 3



749

750 **Figure 3.** Evolution of the SSA_{CR} (A) and WRV (B) with the CD, and WRV with the

751 SSA_{CR} of the LCMNF (C).

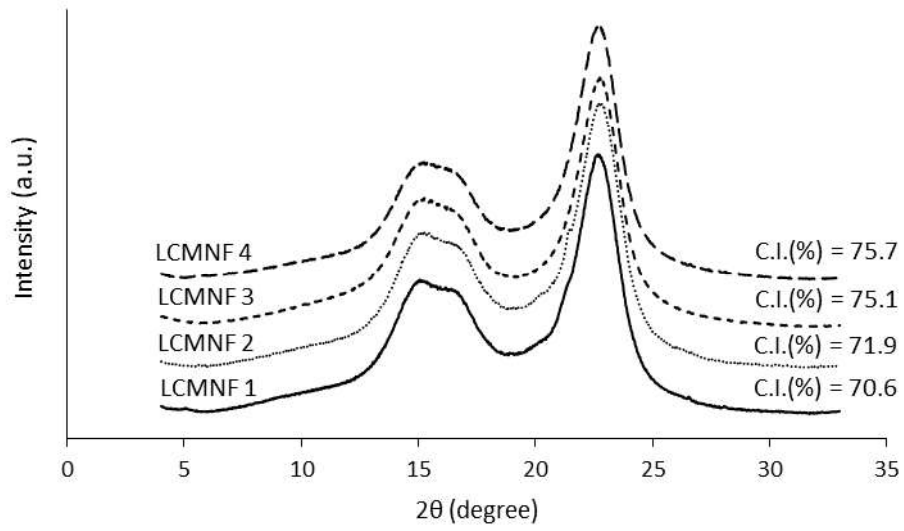
752

753 **Figure 4**

754 - Journal: International Journal of Biological Macromolecules

755 - Author: Ferran Serra-Parareda

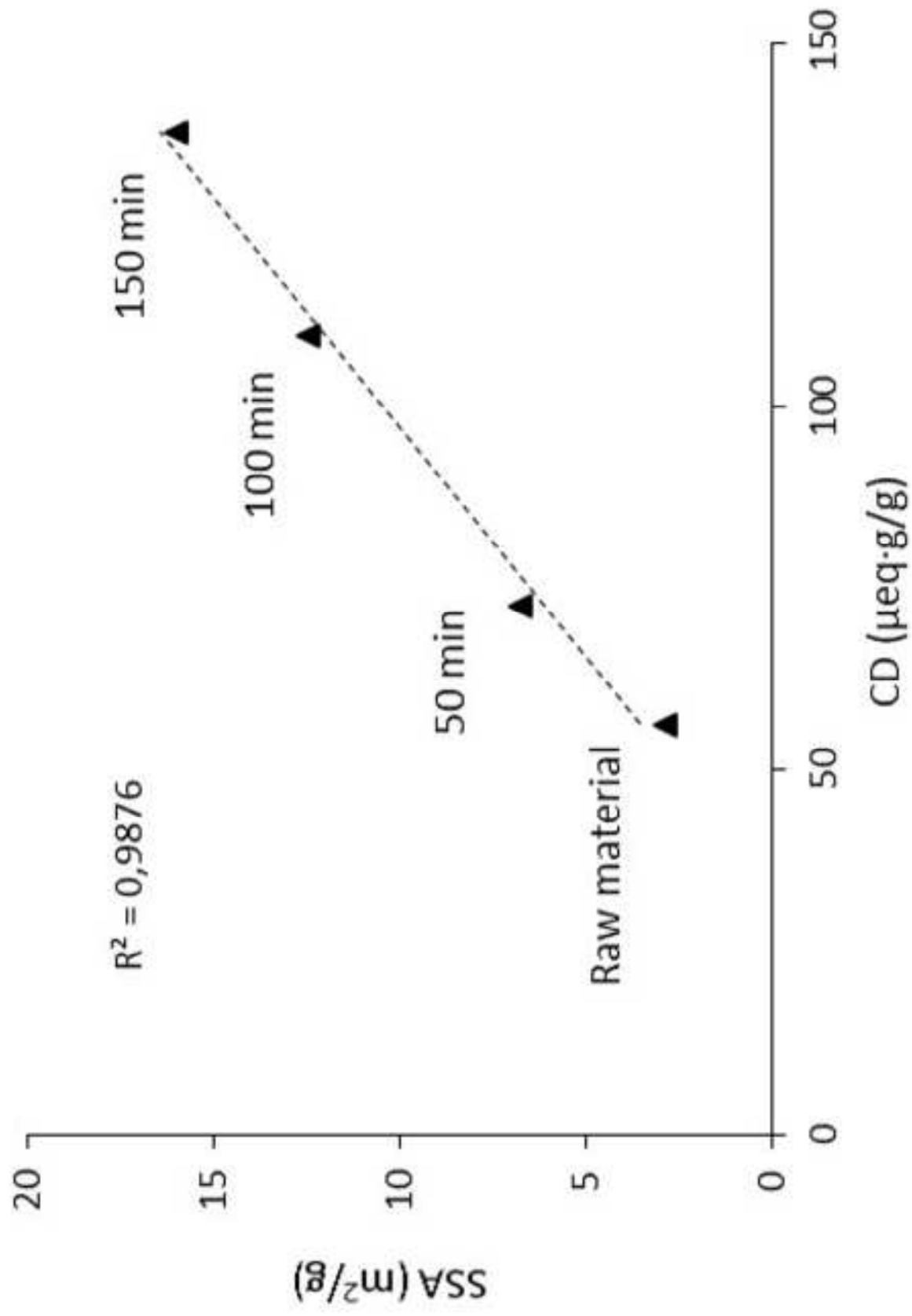
756 - Illustration number: 4

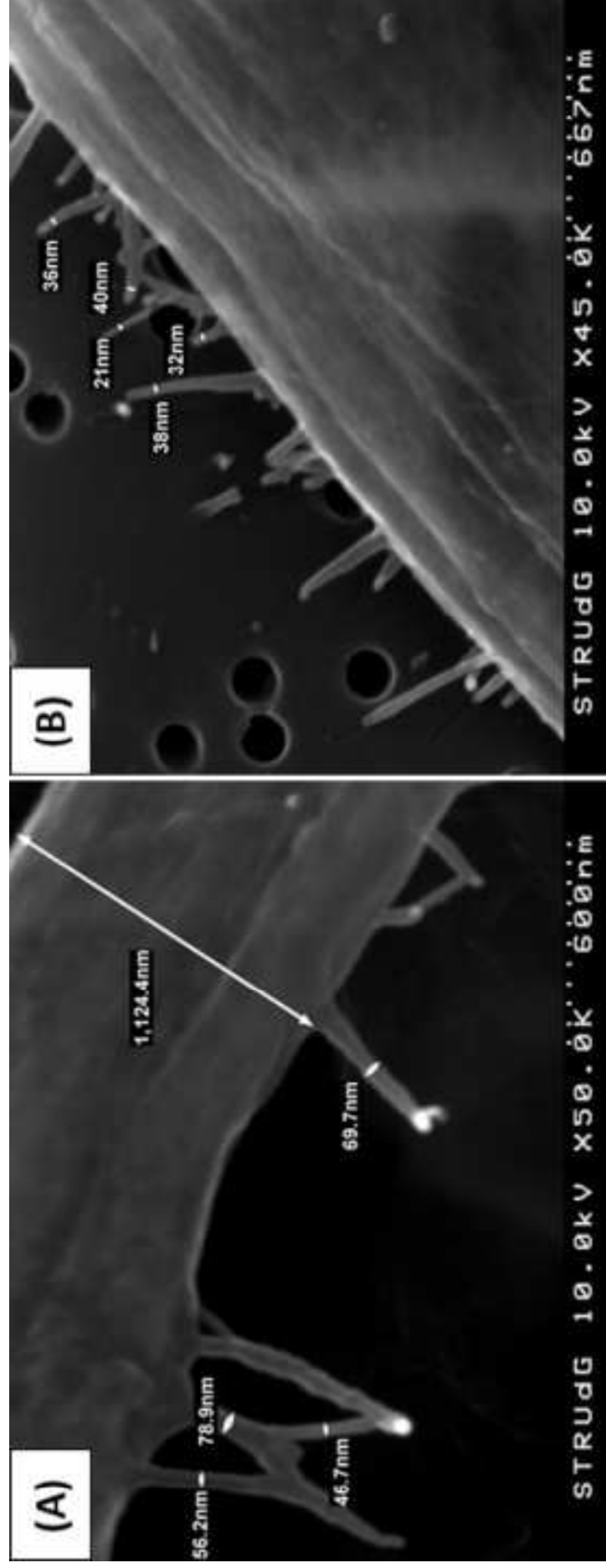


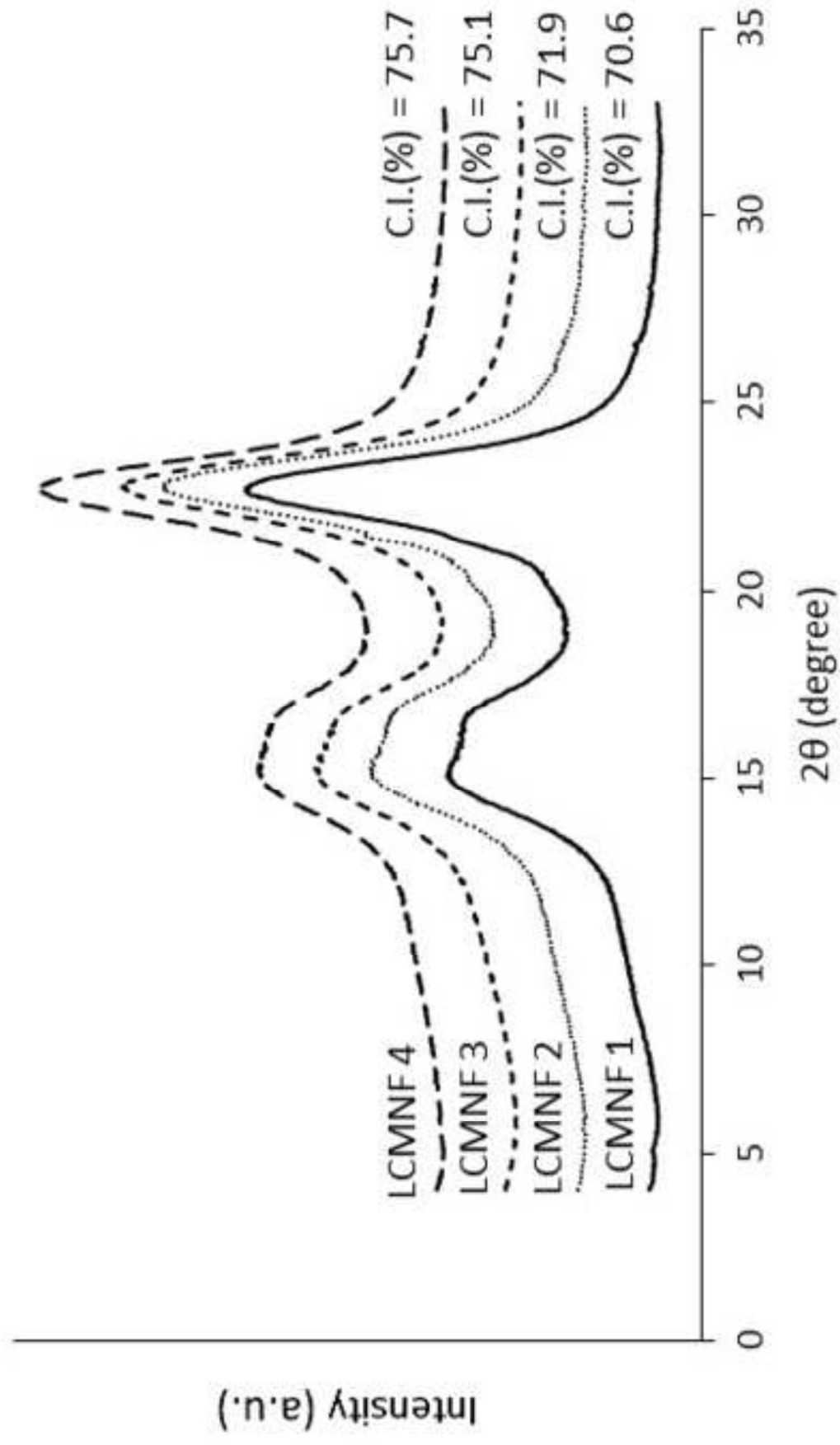
757

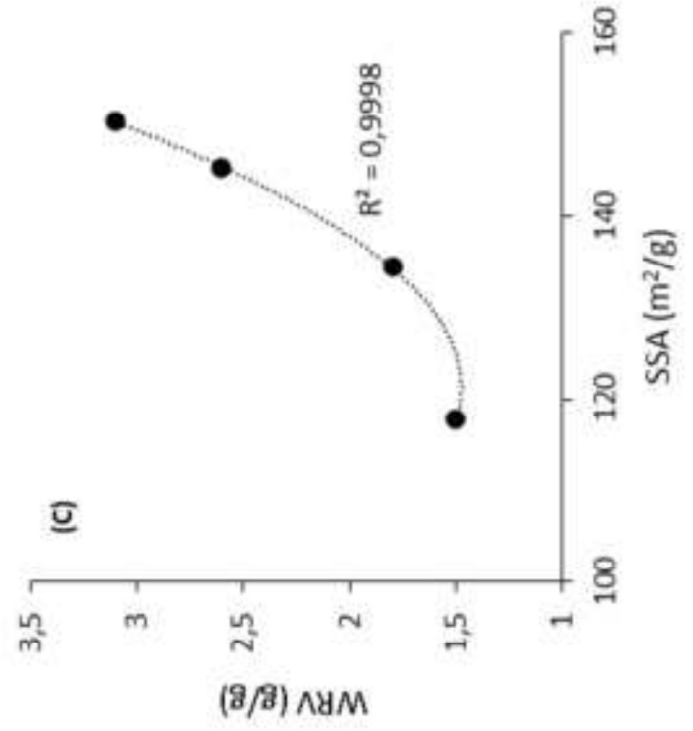
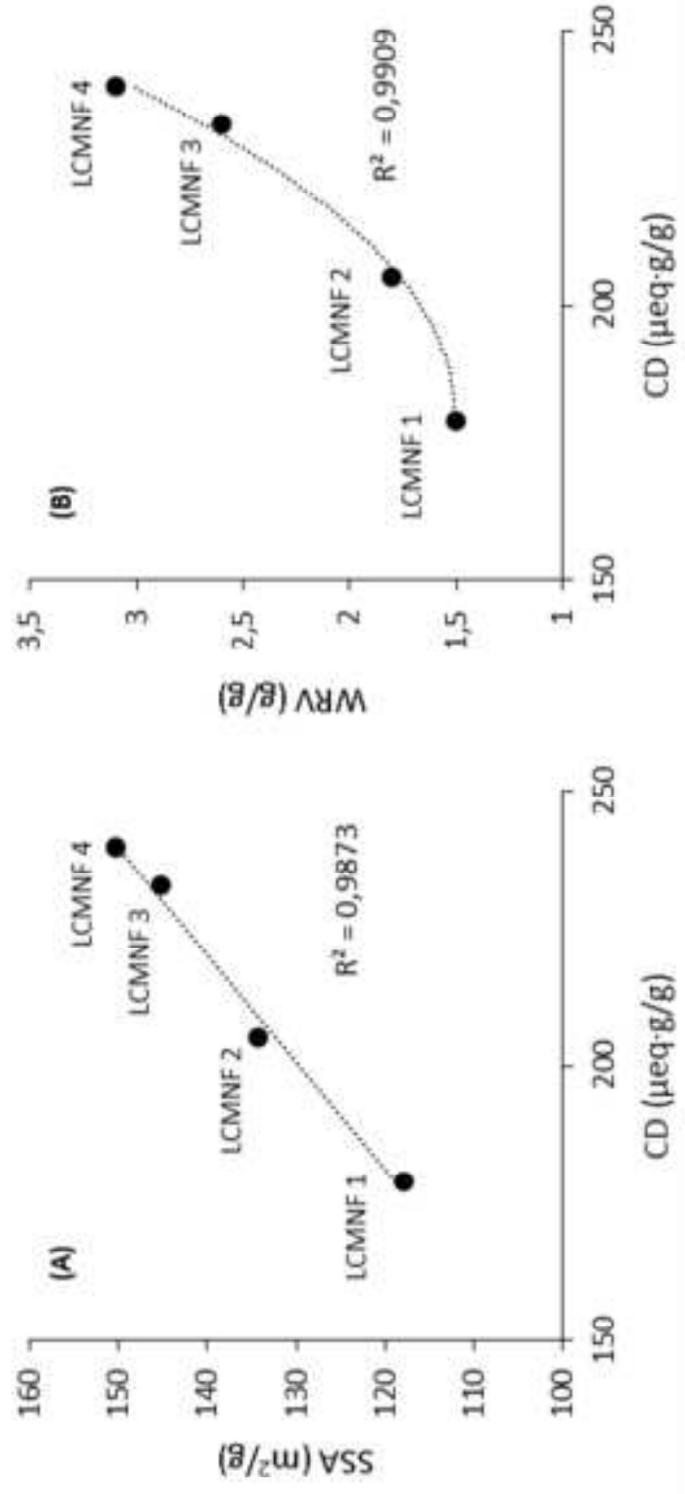
758

Figure 4. XRD analysis of the LCMNF









Declaration of interests

The authors declare that they have no known competing financial interests or personal relationships that could have appeared to influence the work reported in this paper.

The authors declare the following financial interests/personal relationships which may be considered as potential competing interests: